

## Exploring the Dynamics of Zr-Based Metal-organic Frameworks Containing Mechanically Interlocked Molecular Shuttles

Benjamin H. Wilson<sup>a,b†</sup>, Ghazale Gholami<sup>a†</sup>, Kelong Zhu<sup>c</sup>, Christopher A. O’Keefe<sup>d</sup>, Robert W. Schurko<sup>\*d</sup> and Stephen J. Loeb<sup>\*a</sup>

<sup>a</sup> Department of Chemistry and Biochemistry, University of Windsor, Windsor, Ontario, Canada N9B 3P4

<sup>b</sup> Discussion presenter.

<sup>c</sup> School of Chemistry, Sun Yat-Sen University, Guangzhou, P. R. China, 510275

<sup>d</sup> Department of Chemistry and Biochemistry, Florida State University, Tallahassee, FL 32306-4390

Table of Contents	Page
<sup>1</sup> H and <sup>13</sup> C NMR Spectra of <b>2</b>	S2
<sup>1</sup> H and <sup>13</sup> C NMR Spectra of <b>3</b>	S3
<sup>1</sup> H and <sup>13</sup> C NMR Spectra of [H <b>3</b> ][BF <sub>4</sub> ]	S4
<sup>1</sup> H and <sup>13</sup> C NMR Spectra of <b>4</b>	S5
<sup>1</sup> H and <sup>13</sup> C NMR Spectra of H <sub>4</sub> <b>5</b>	S6
<sup>1</sup> H and <sup>13</sup> C NMR Spectra of <sup>13</sup> C 4-bromobenzaldehyde	S7
<sup>1</sup> H and <sup>13</sup> C NMR Spectra of <b>2</b> *	S8
<sup>1</sup> H and <sup>13</sup> C NMR Spectra of <b>3</b> *	S9
<sup>1</sup> H and <sup>13</sup> C NMR Spectra of [H <b>3</b> *][BF <sub>4</sub> ]	S10
<sup>1</sup> H and <sup>13</sup> C NMR Spectra of <b>4</b> *	S11
<sup>1</sup> H and <sup>13</sup> C NMR Spectra of H <sub>4</sub> <b>5</b> *	S12
Comparison of <sup>13</sup> C NMR Spectra for <b>4</b> and <b>4</b> *	S13
<sup>1</sup> H and <sup>13</sup> C NMR Spectra of <b>4</b> *, [H <b>4</b> *][BF <sub>4</sub> ] and [H <sub>2</sub> <b>4</b> *][BF <sub>4</sub> ] <sub>2</sub>	S13
Determination of Shuttling Rates (Solution) for <b>4</b> * and [H <sub>2</sub> <b>4</b> *][BF <sub>4</sub> ] <sub>2</sub>	S14
Solution <sup>1</sup> H NMR Spectra of Digested MOFs	S17
SSNMR Spectra for <b>UWDM-8</b> and <b>PCN-57</b>	S19
Synthesis of different protonation states of <b>4</b> * and <b>UWDM-8</b>	S19
VT-PXRD of <b>UWDM-8</b> and <b>UWDM-9</b>	S20
VT <sup>13</sup> C MAS SSNMR Spectra of <b>UWDM-8</b> and <b>UWDM-9</b>	S20
References	S21

# $^1\text{H}$ NMR and $^{13}\text{C}$ NMR Spectra

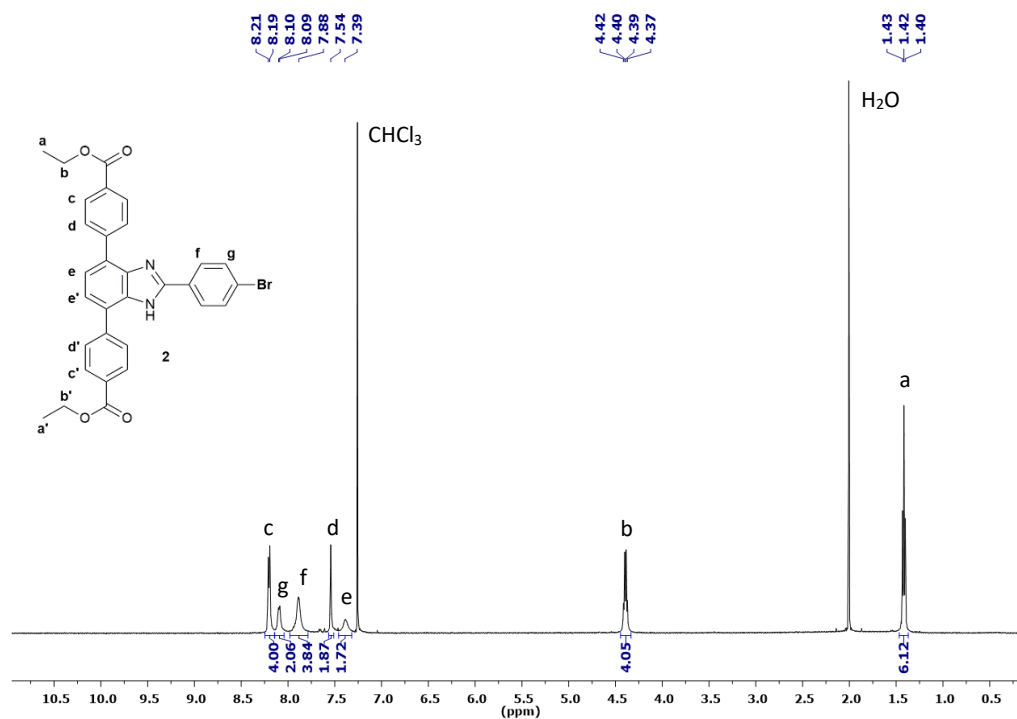


Figure S1.  $^1\text{H}$  NMR spectrum of Compound 2 (500 MHz,  $\text{CDCl}_3$ , 298 K)

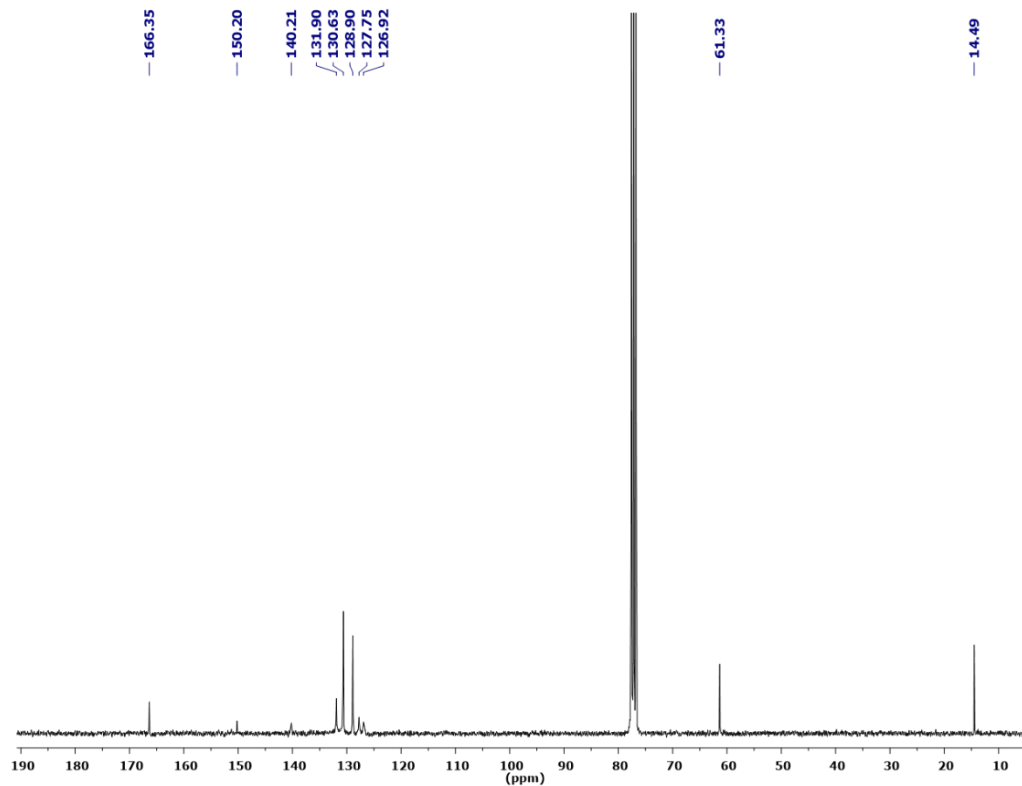


Figure S2.  $^{13}\text{C}$  NMR spectrum of Compound 2 (125 MHz,  $\text{CDCl}_3$ , 298 K)

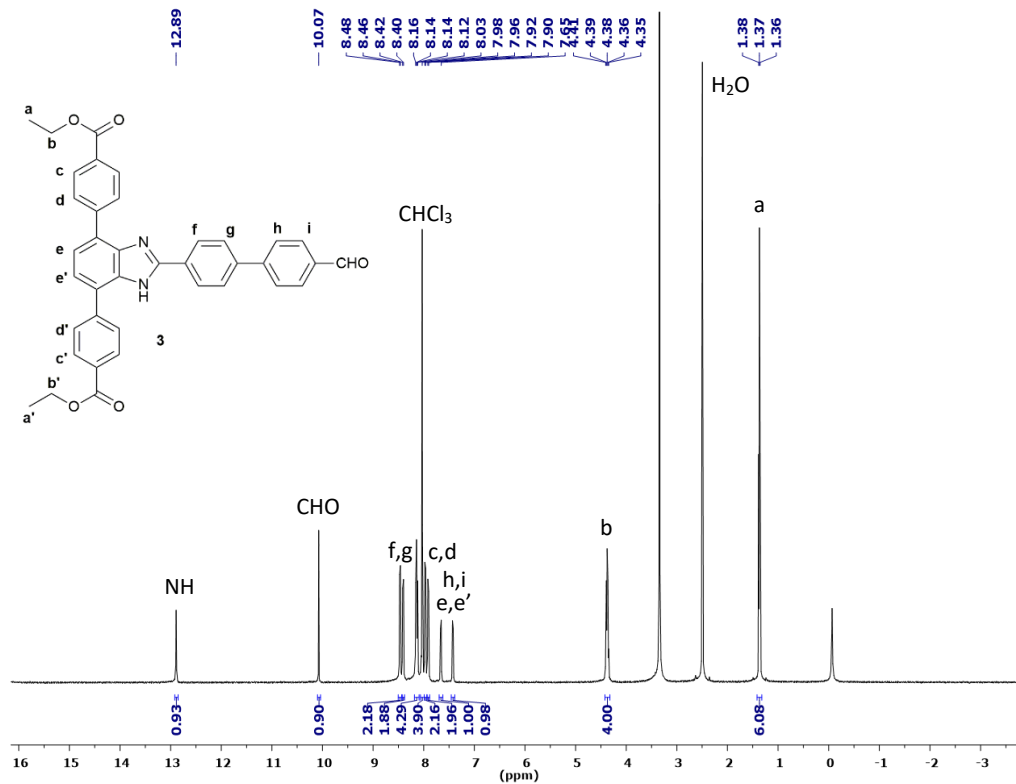


Figure S3.  $^1\text{H}$  NMR spectrum of Compound 3 (500 MHz,  $\text{CDCl}_3$ , 298 K)

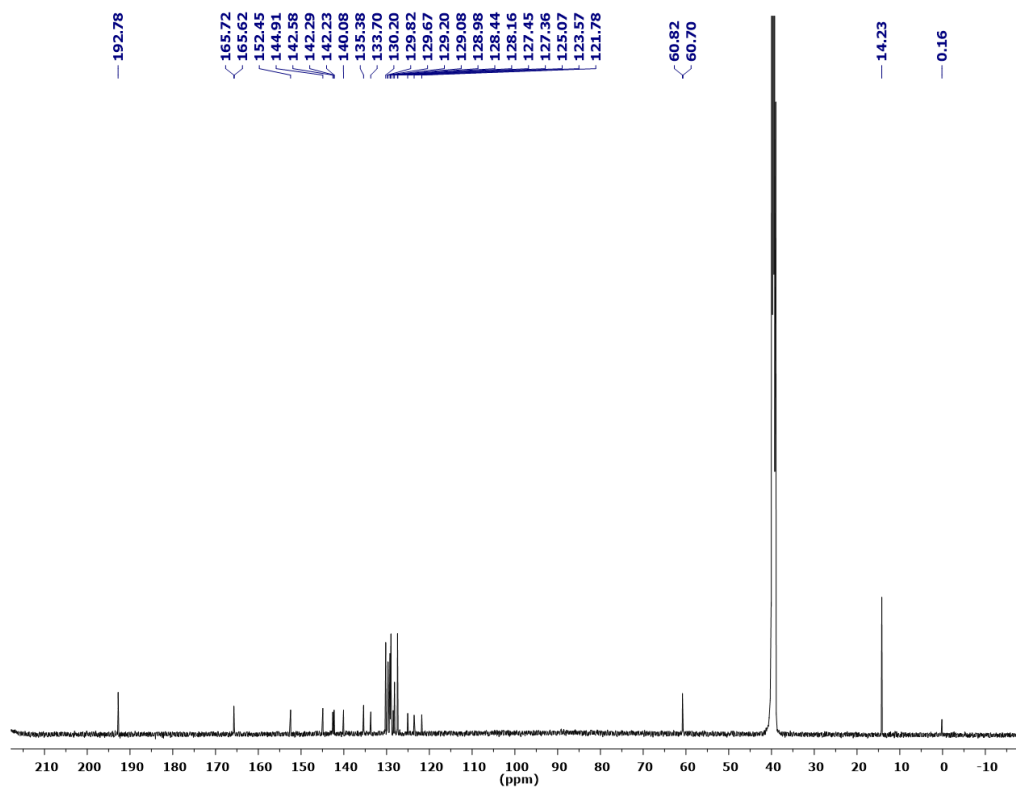


Figure S4.  $^{13}\text{C}$  NMR spectrum of Compound 3 (125 MHz,  $\text{CDCl}_3$ , 298 K)

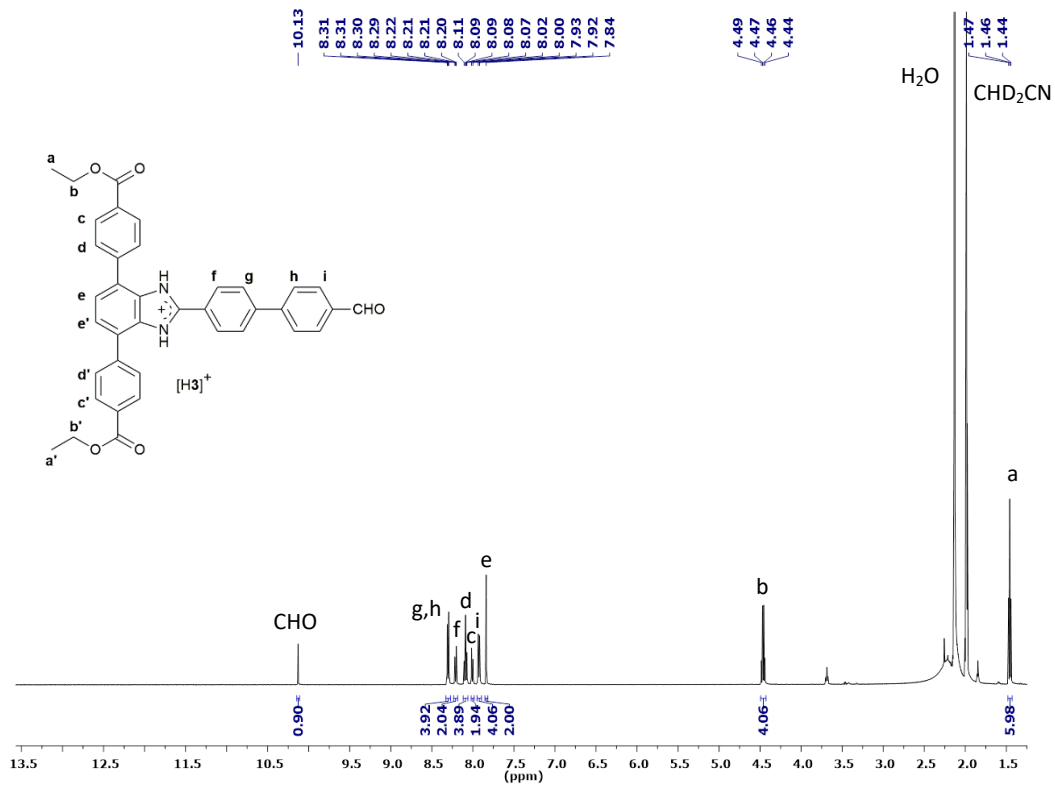


Figure S5. <sup>1</sup>H NMR spectrum of Compound [H3][BF<sub>4</sub>] (500 MHz, CD<sub>3</sub>CN, 298 K)

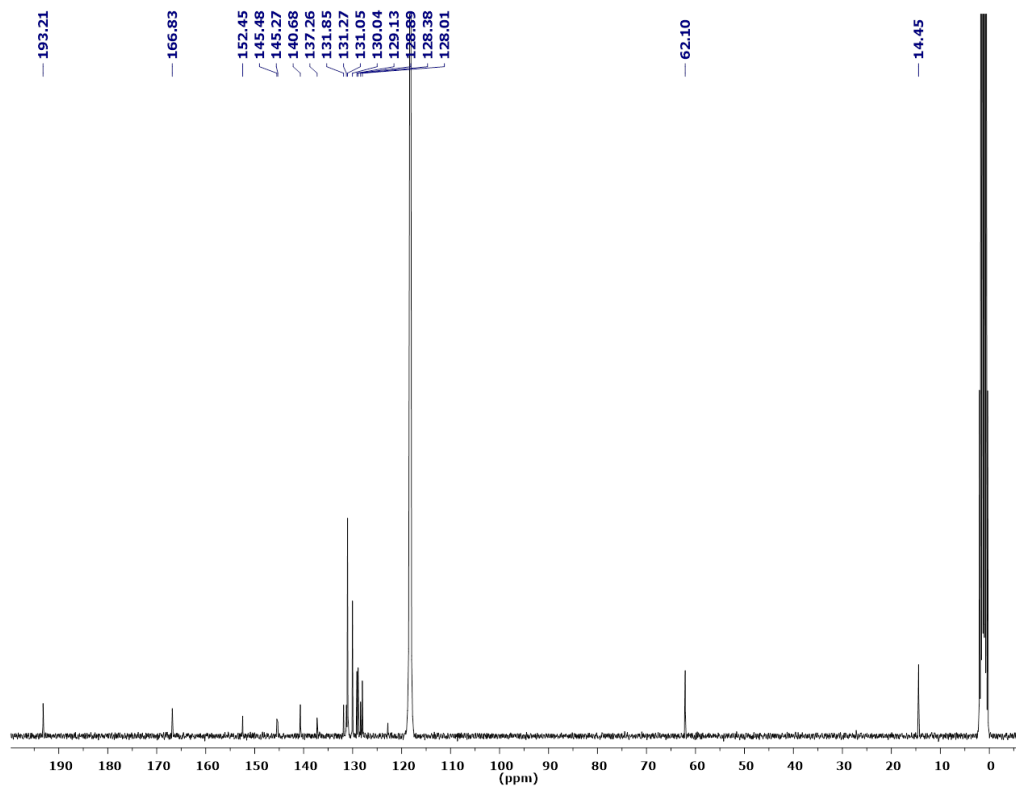


Figure S6. <sup>13</sup>C NMR spectrum of Compound [H3][BF<sub>4</sub>] (125 MHz, CD<sub>3</sub>CN, 298 K)

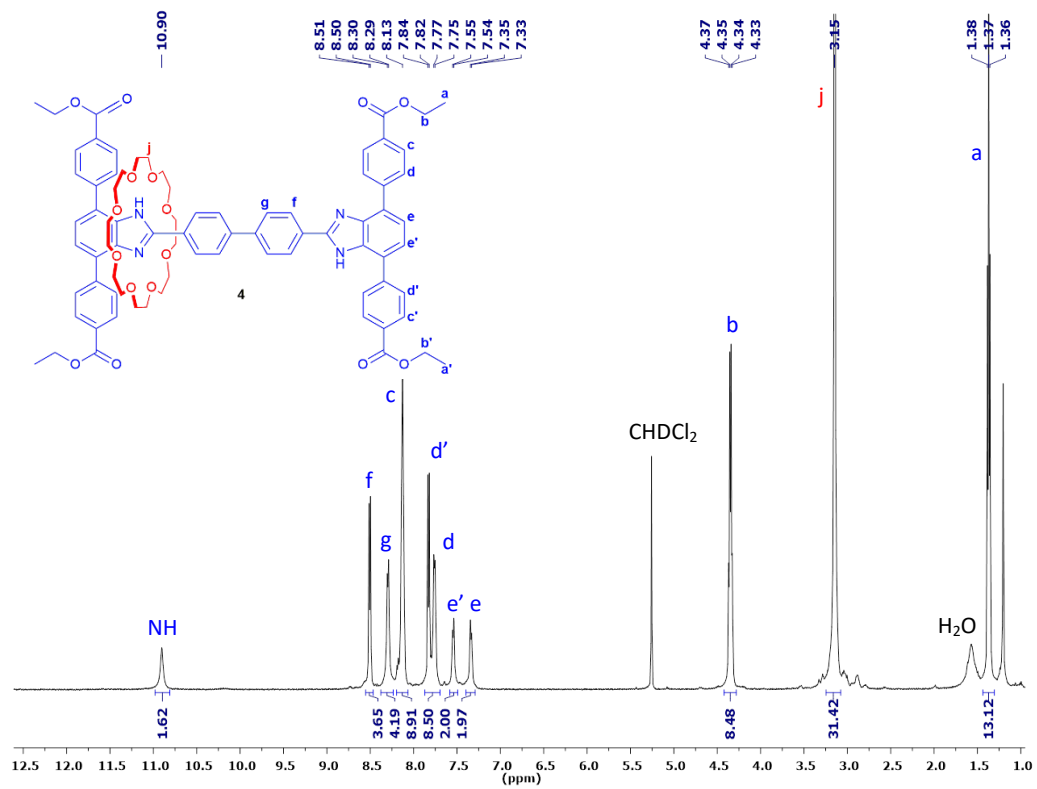


Figure S7.  $^1\text{H}$  NMR spectrum of Compound 4 (500 MHz,  $\text{CD}_2\text{Cl}_2$ , 298 K)

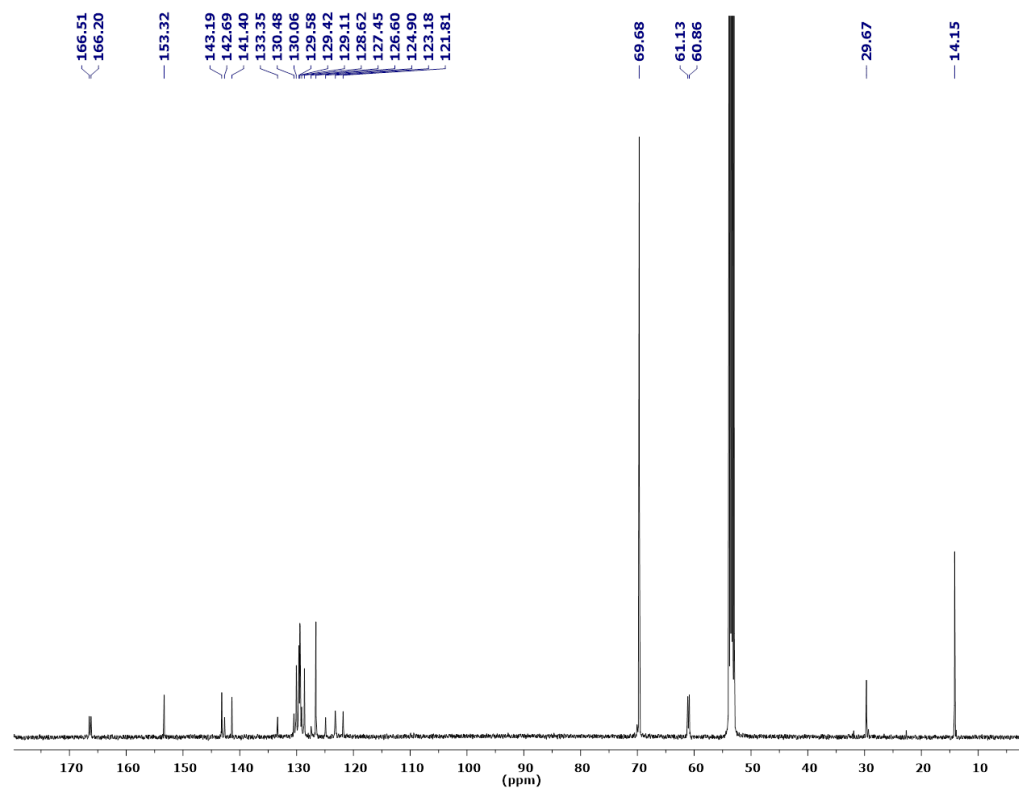


Figure S8.  $^{13}\text{C}$  NMR spectrum of Compound 4 (125 MHz,  $\text{CD}_2\text{Cl}_2$ , 298 K)

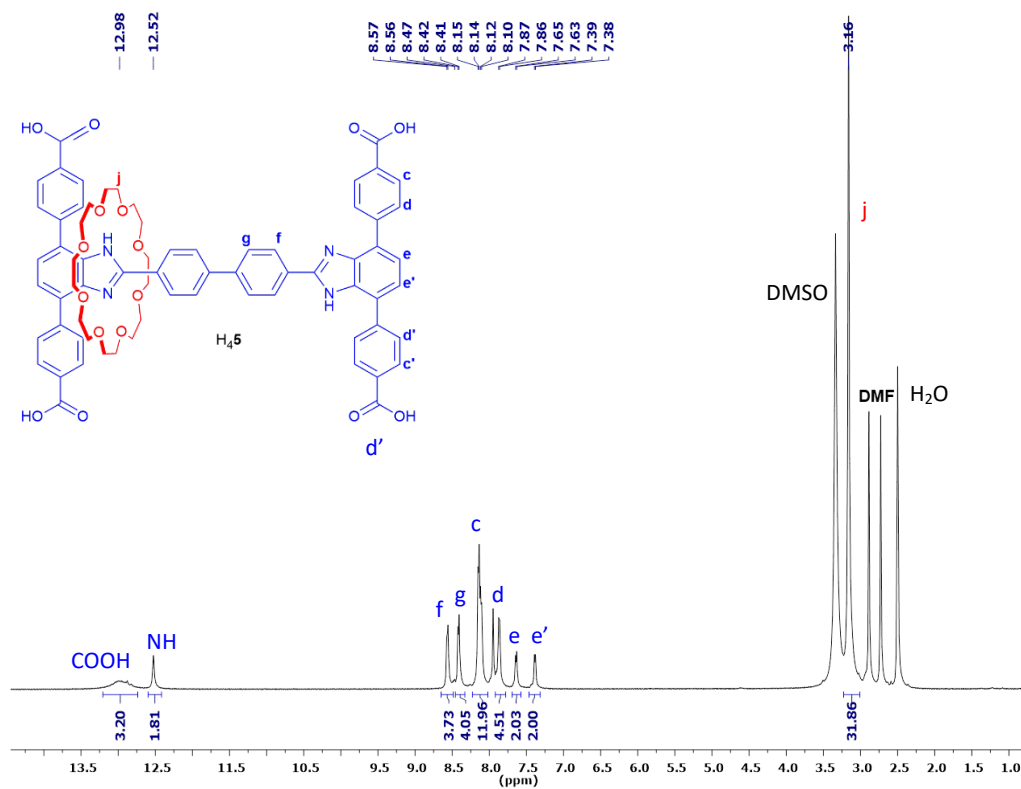


Figure S9. <sup>1</sup>H NMR spectrum of Compound H<sub>4</sub>5 (500 MHz, d<sub>6</sub>-DMSO, 298 K)

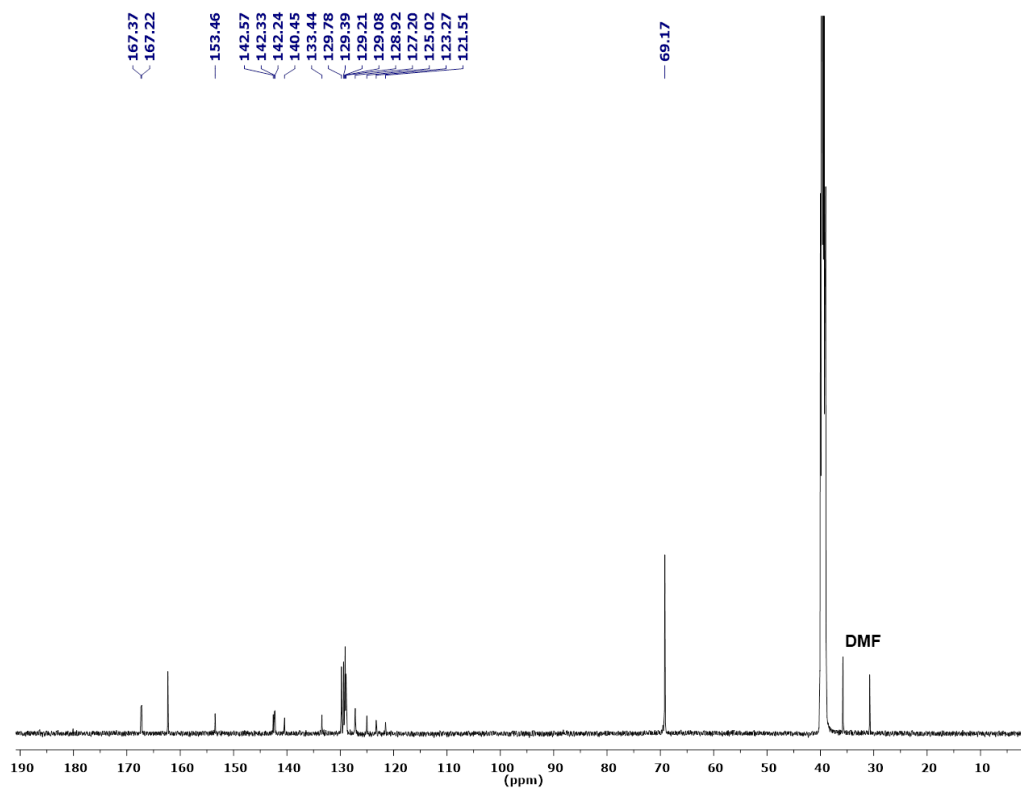
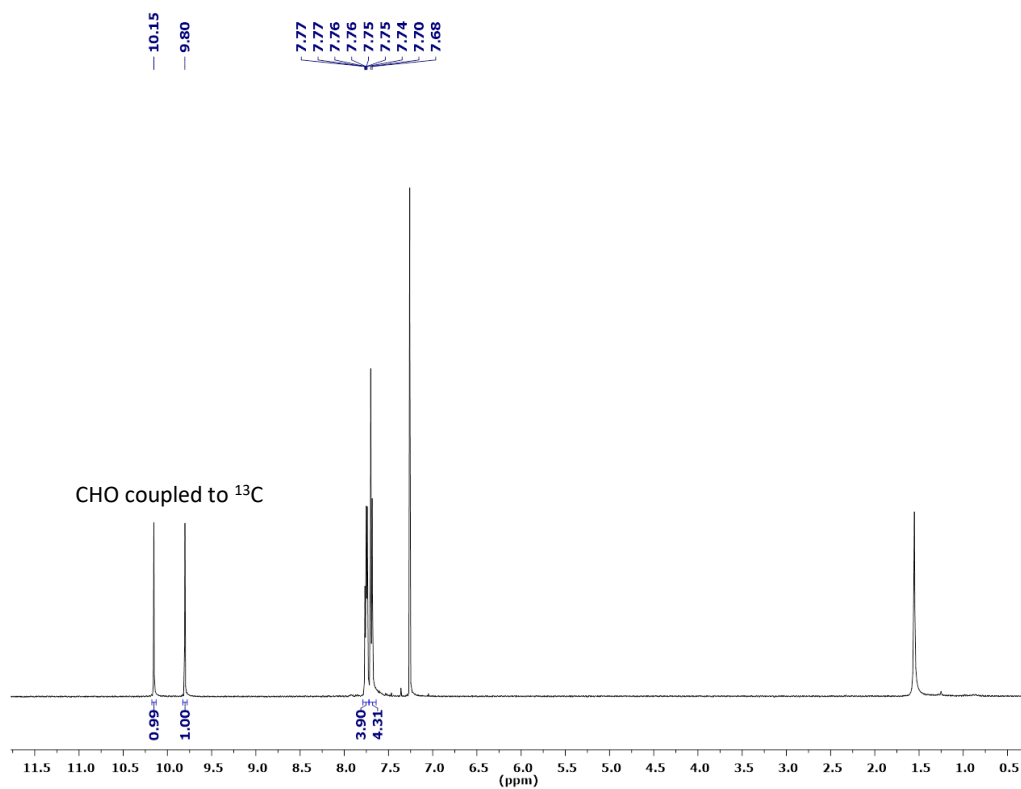
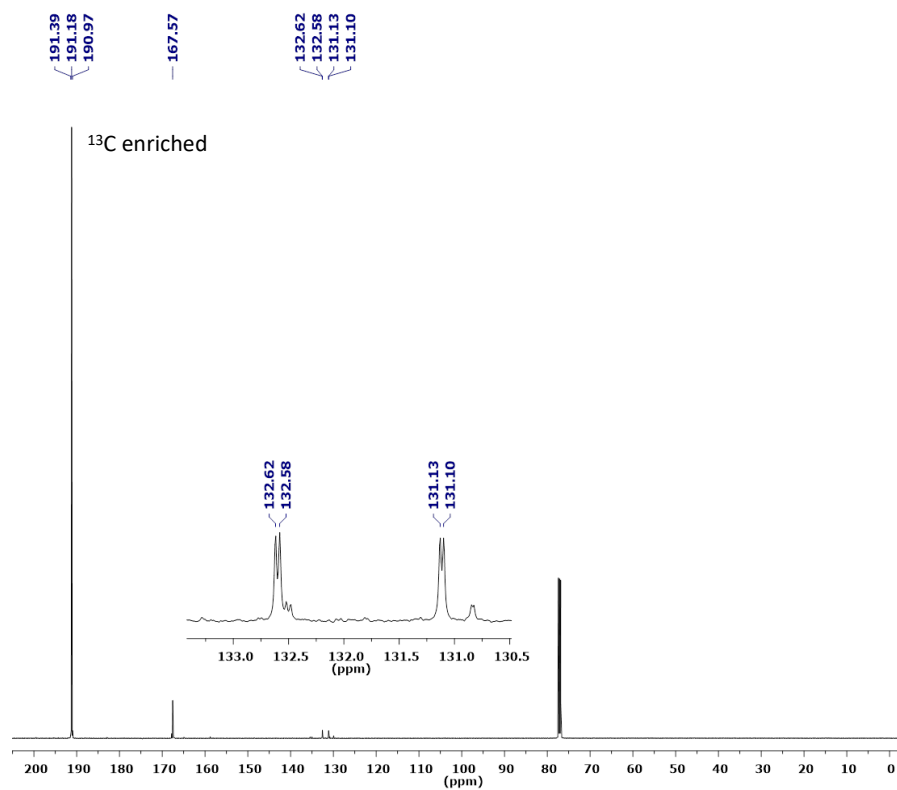


Figure S10. <sup>13</sup>C NMR spectrum of Compound H<sub>4</sub>5 (125 MHz, d<sub>6</sub>-DMSO, 298 K)



**Figure S11.**  $^1\text{H}$  NMR spectrum of  $^{13}\text{C}$  4-bromobenzaldehyde (500 MHz,  $\text{CDCl}_3$ , 298 K)



**Figure S12.**  $^{13}\text{C}$  NMR spectrum of  $^{13}\text{C}$  4-bromobenzaldehyde (125 MHz,  $\text{CDCl}_3$ , 298 K)

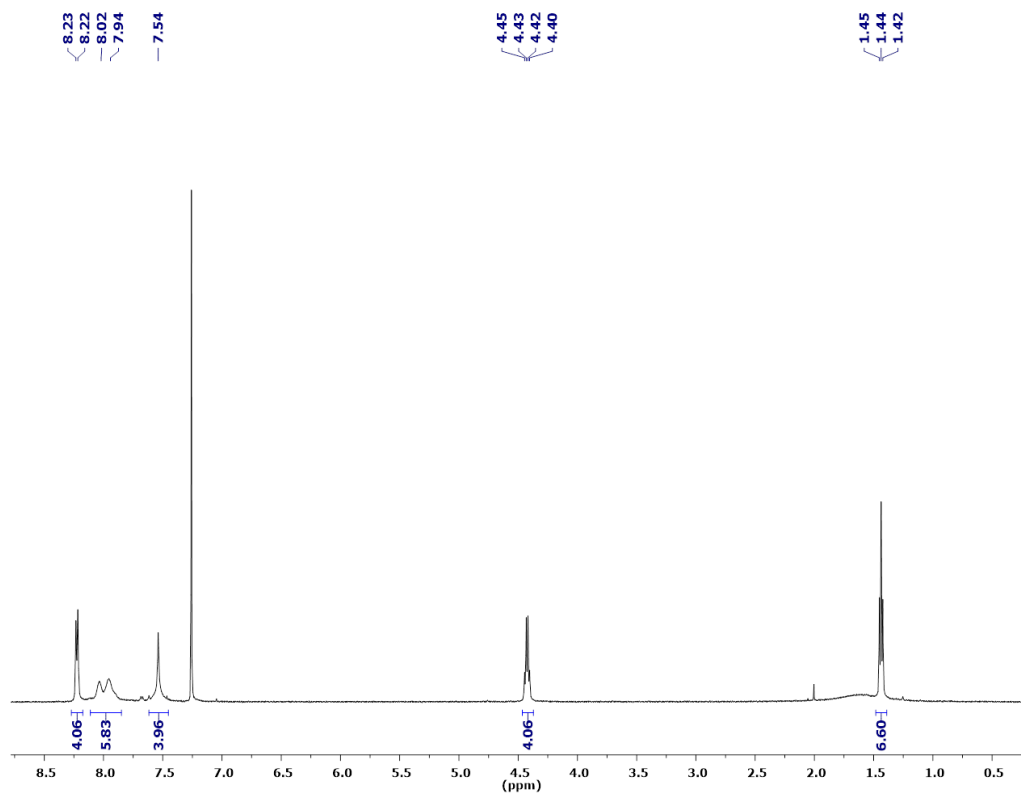


Figure S13.  $^1\text{H}$  NMR spectrum of Compound 2\* (500 MHz,  $\text{CDCl}_3$ , 298 K)

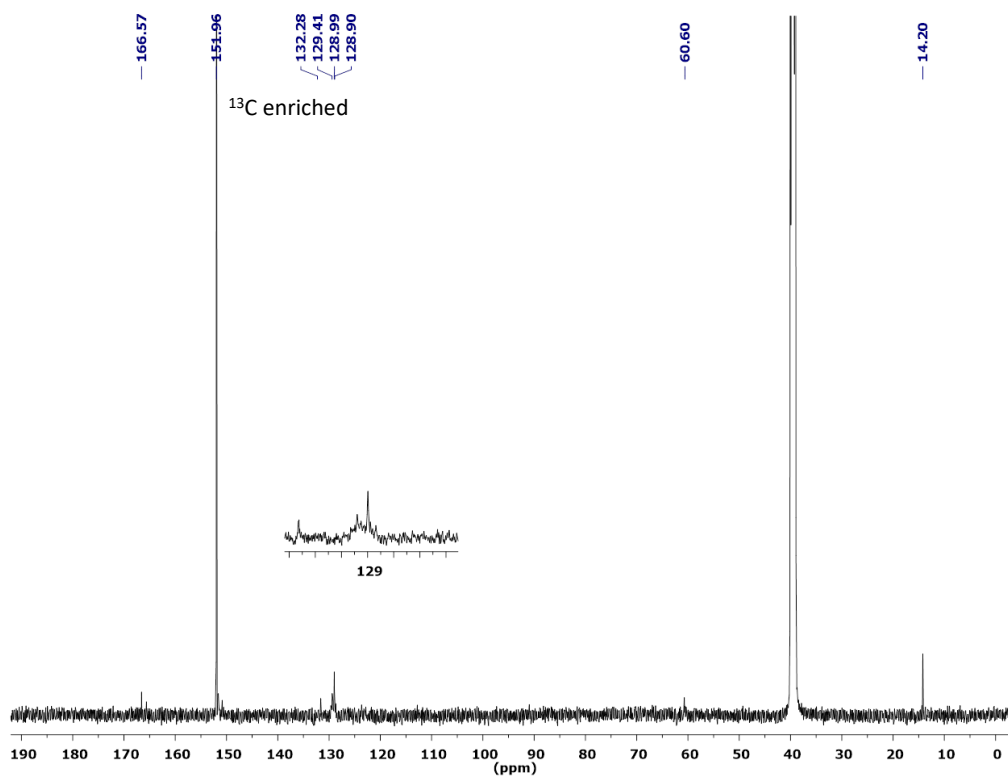


Figure S14.  $^{13}\text{C}$  NMR spectrum of Compound 2\* (125 MHz,  $\text{CDCl}_3$ , 298 K)



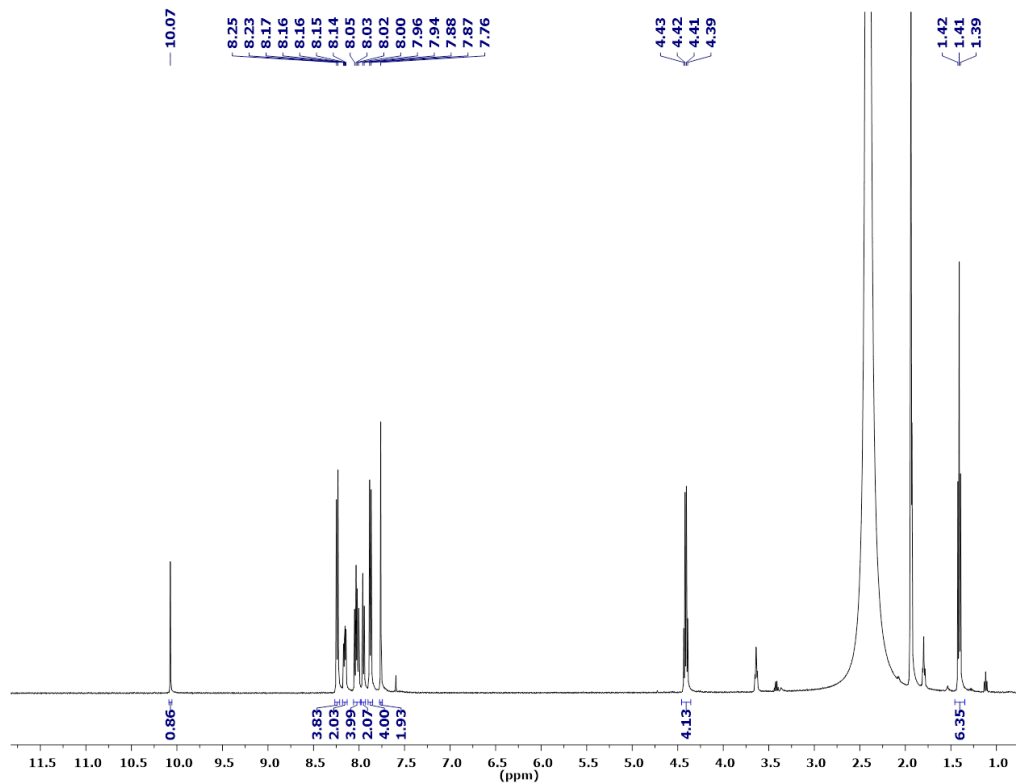


Figure S15. <sup>1</sup>H NMR spectrum of Compound 3\* (500 MHz, CDCl<sub>3</sub>, 298 K)

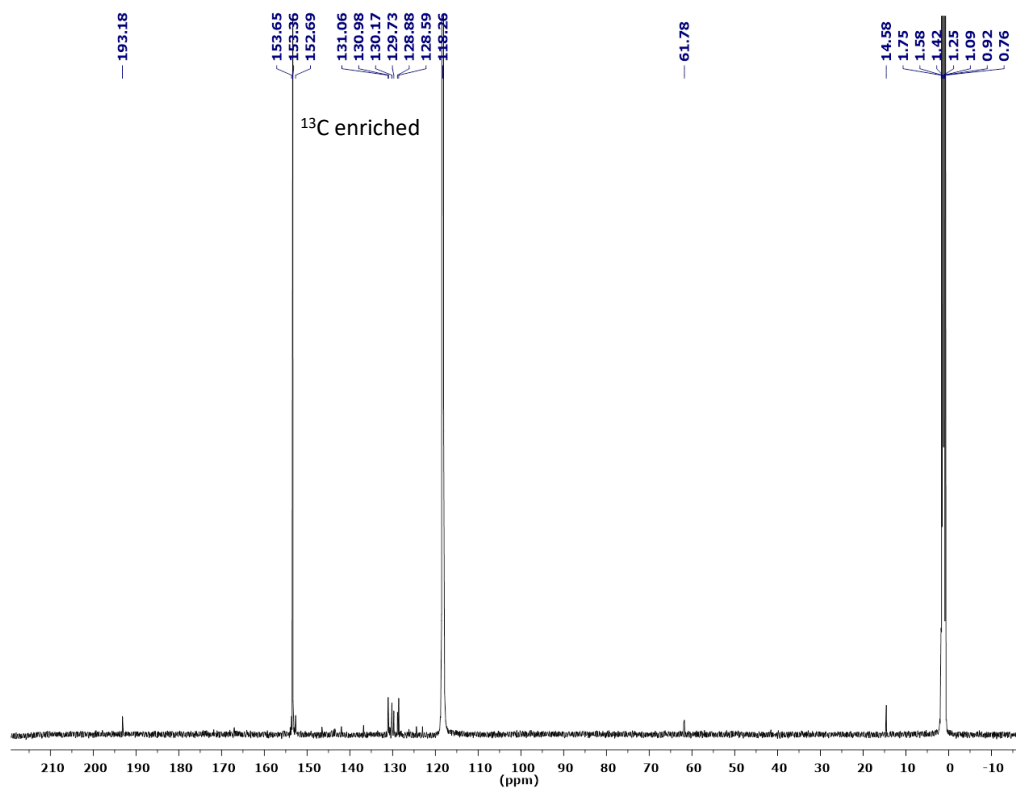


Figure S16. <sup>13</sup>C NMR spectrum of Compound 3\* (125 MHz, CDCl<sub>3</sub>, 298 K)

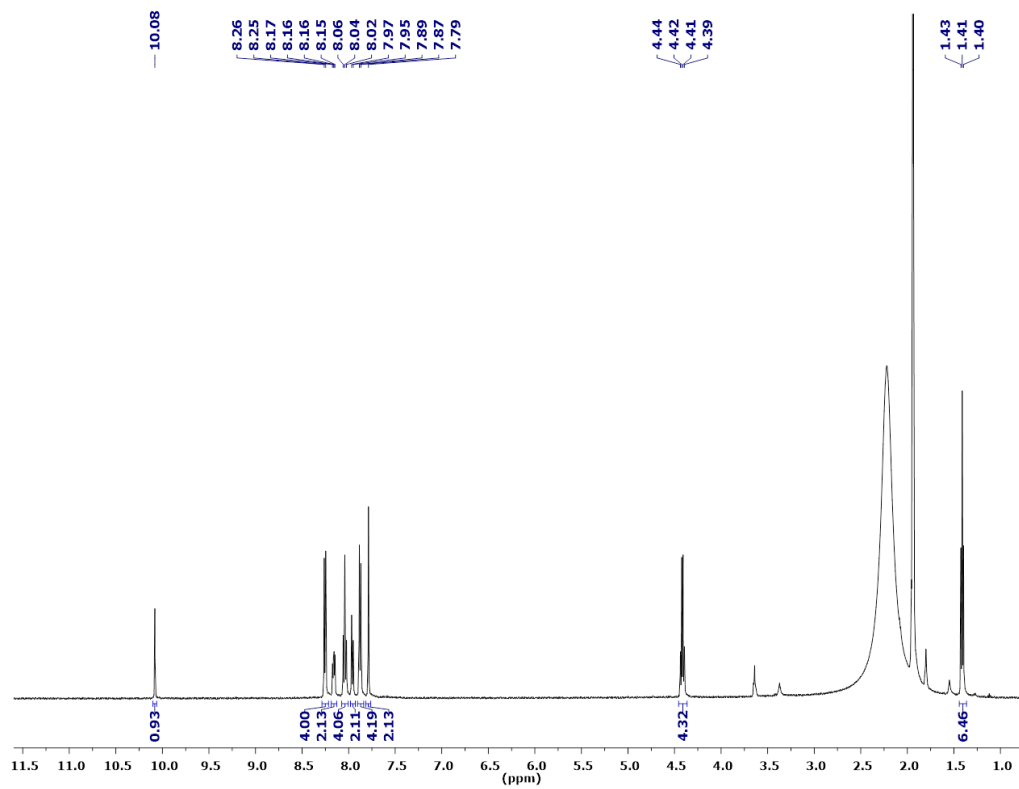


Figure S17.  $^1\text{H}$  NMR spectrum of Compound  $[\text{H3}^*][\text{BF}_4]$  (500 MHz,  $\text{CD}_3\text{CN}$ , 298 K)

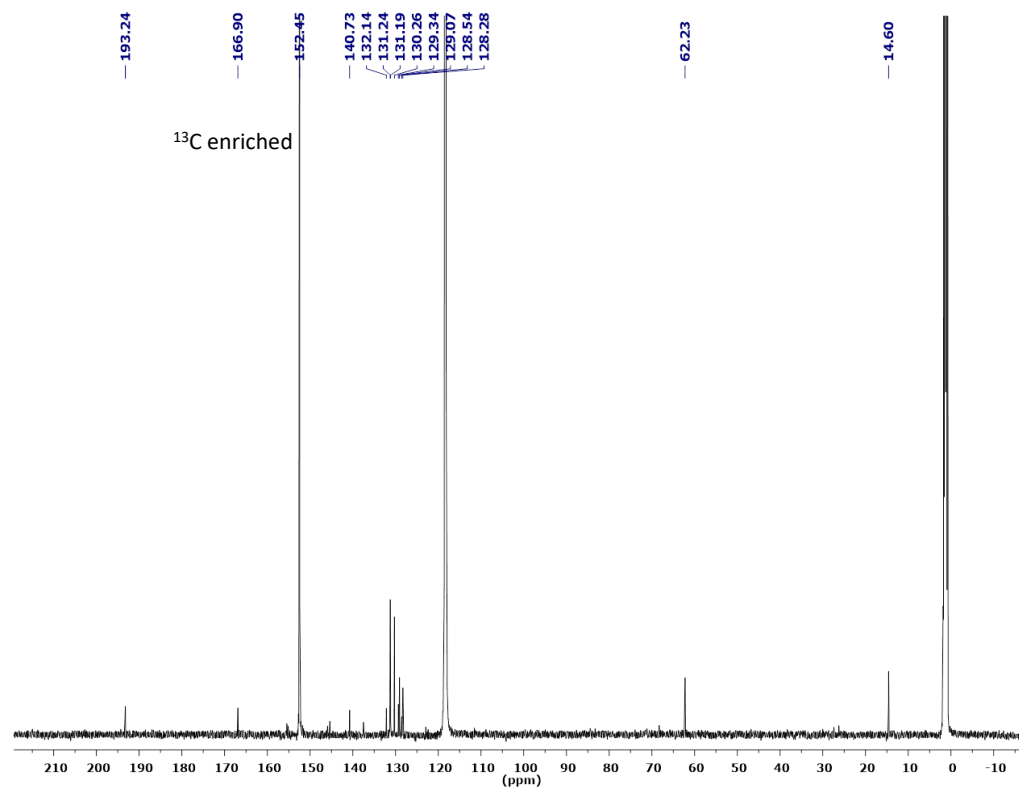


Figure S18.  $^{13}\text{C}$  NMR spectrum of Compound  $[\text{H3}^*][\text{BF}_4]$  (125 MHz,  $\text{CD}_3\text{CN}$ , 298 K)

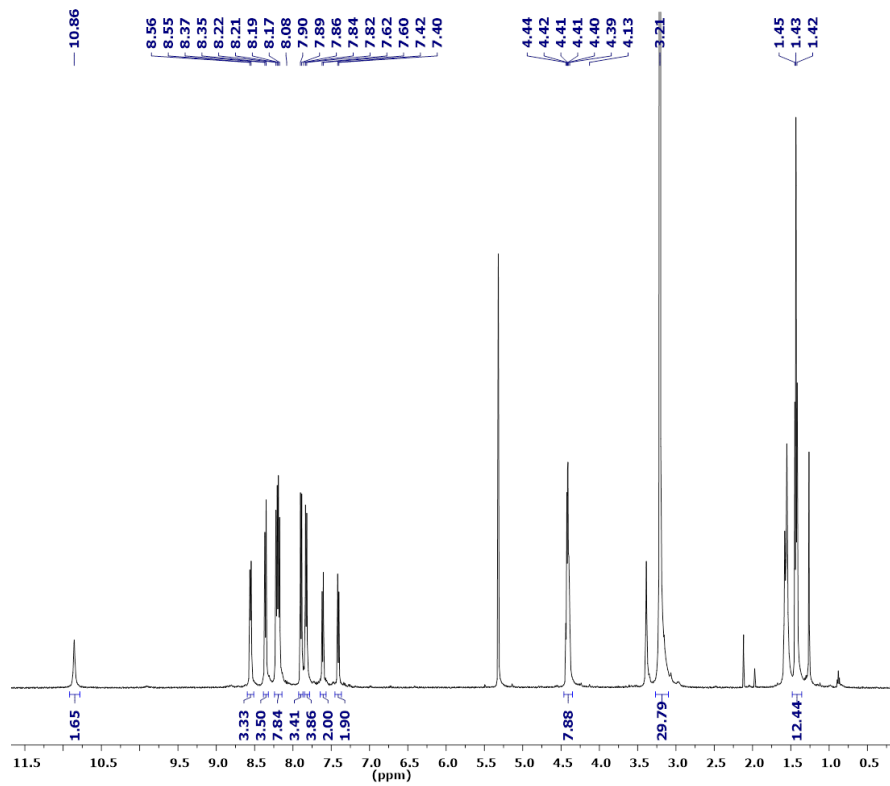


Figure S19.  $^1\text{H}$  NMR spectrum of Compound **4\*** (500 MHz,  $\text{CD}_2\text{Cl}_2$ , 298 K)

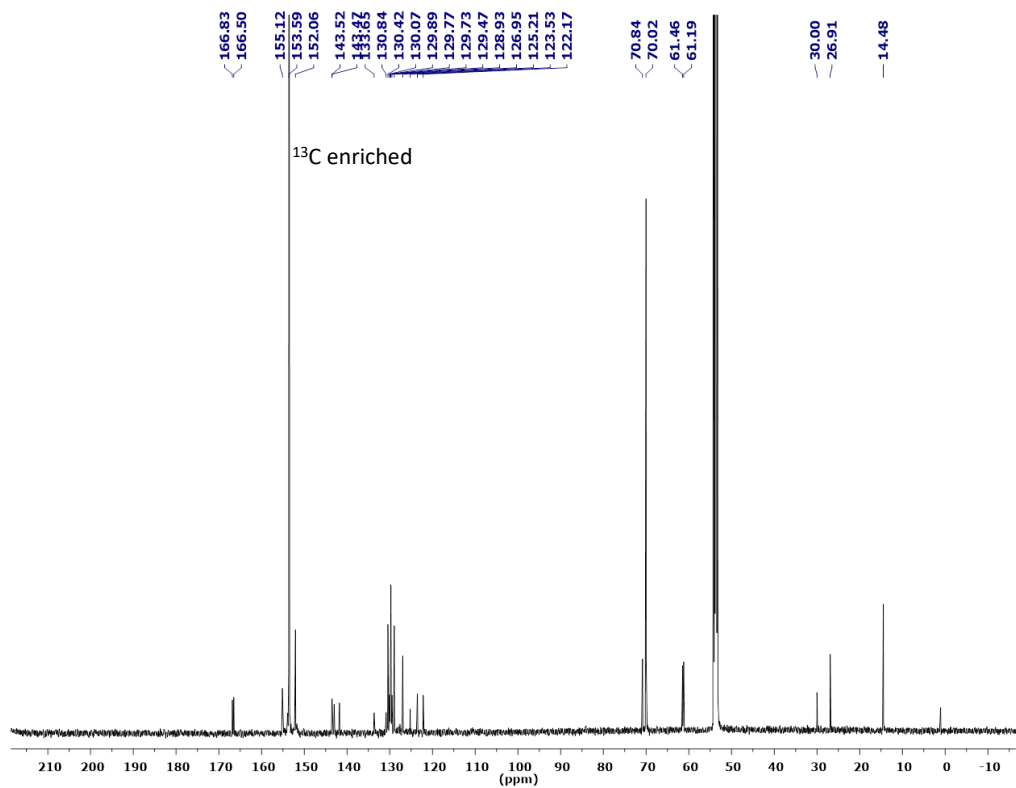
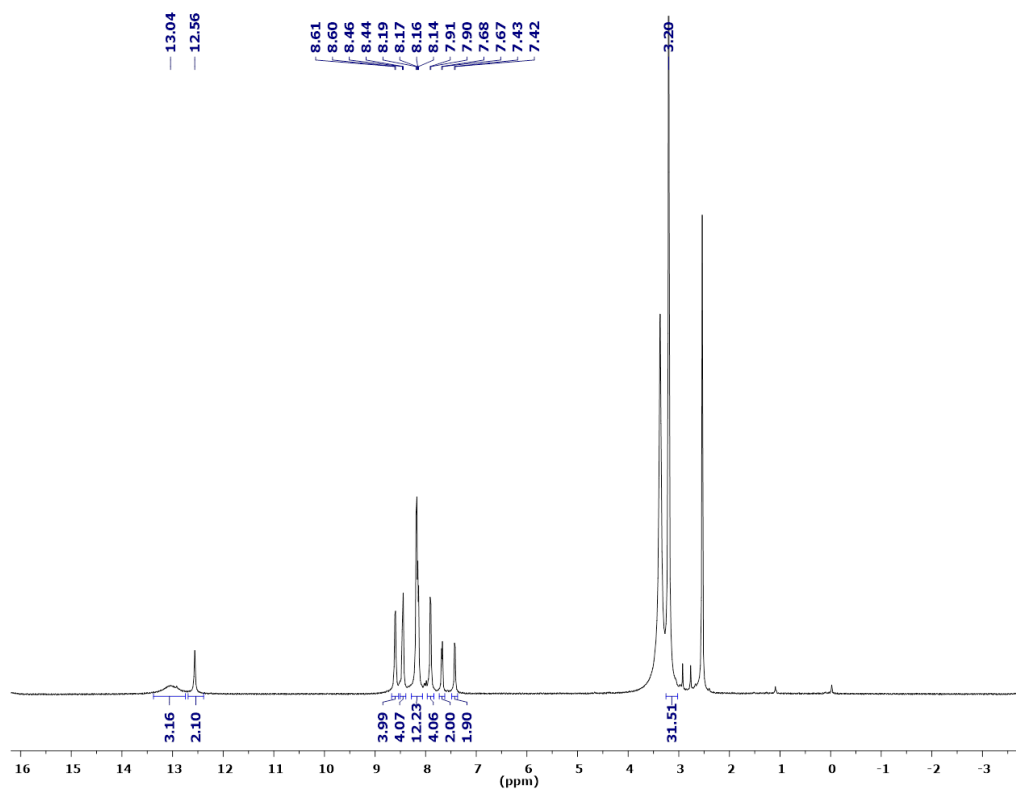
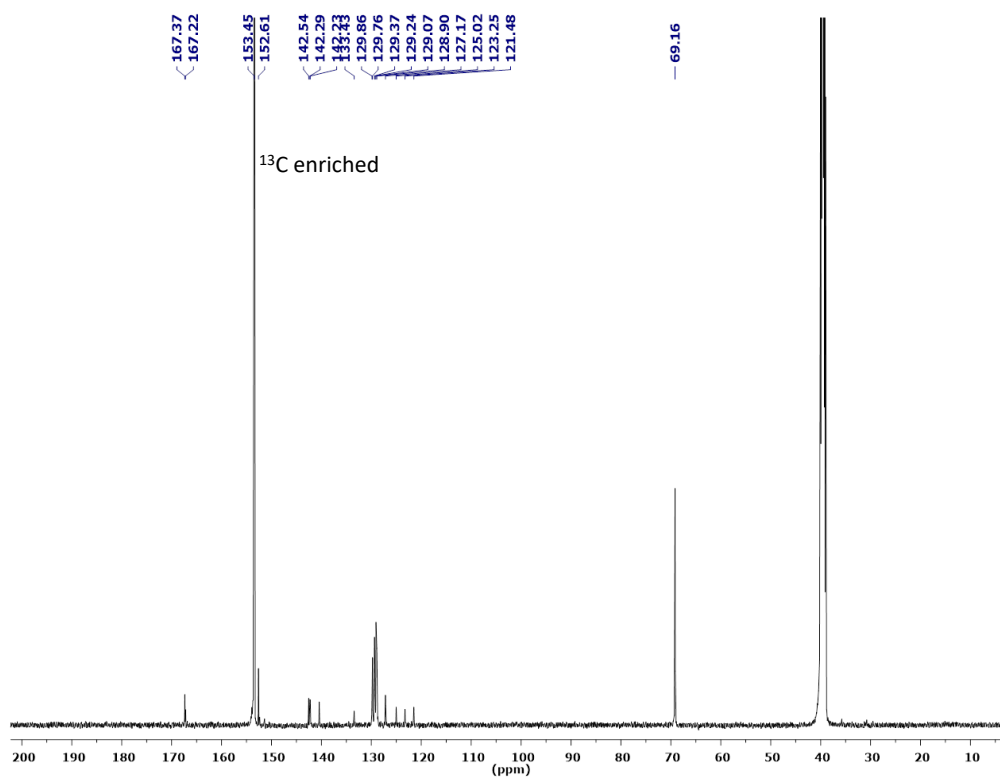


Figure S20.  $^{13}\text{C}$  NMR spectrum of Compound **4\*** (125 MHz,  $\text{CD}_2\text{Cl}_2$ , 298 K)



**Figure S21.**  $^1\text{H}$  NMR spectrum of Compound  $\text{H}_4\text{5}^*$  (500 MHz,  $d_6$ -DMSO, 298 K)



**Figure S22.**  $^{13}\text{C}$  NMR spectrum of Compound  $\text{H}_4\text{5}^*$  (125 MHz,  $d_6$ -DMSO, 298 K)

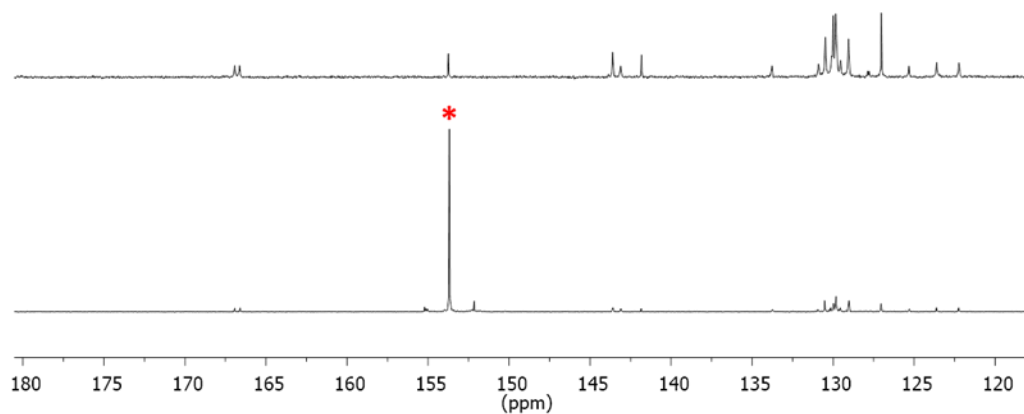


**Figure S23.** Comparison of  $^{13}\text{C}$  NMR spectra of **4** and **4\*** (125 MHz,  $d_6$ -DMSO, 298 K) showing the  $^{13}\text{C}$  enriched carbon environment \*.

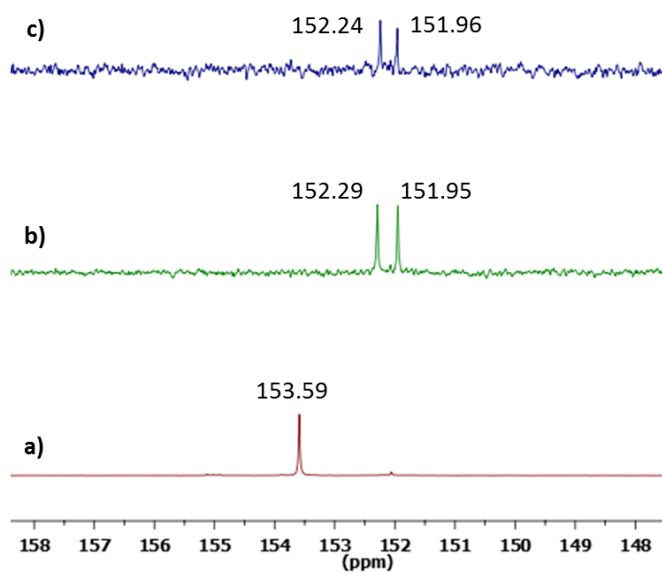


**Figure S24.** Partial  $^{13}\text{C}$  NMR solution spectra (125 MHz,  $\text{CD}_2\text{Cl}_2$ , 298K) of a) **4\*** (neutral rotaxane linker), showing one peak due to fast-exchange of occupied and unoccupied sites, b)  $[\text{H}_4^*]^+$  (+1 charged rotaxane linker) showing that the two sites are different and resolved, one is charged and occupied the other is neutral and unoccupied, c)  $[\text{H}_2\text{4}^*]^{2+}$  (+2 charged rotaxane linker) showing two sites due to slow-exchange of occupied and unoccupied sites.

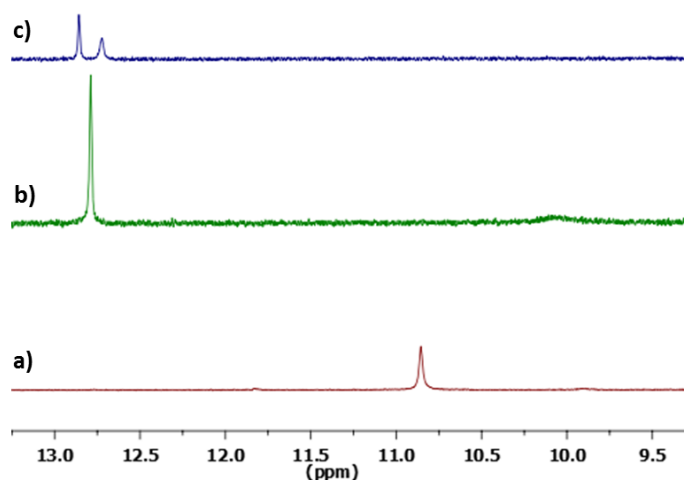


**Figure S25.** Partial  $^1\text{H}$  NMR solution spectra, NH resonances (500 MHz,  $\text{CD}_2\text{Cl}_2$ , 298 K) of a)  $4^*$  (neutral rotaxane linker), showing one peak due to fast-exchange of occupied and unoccupied sites, b)  $[\text{H}4^*]^+$  (+1 charged rotaxane linker) showing that the two sites are different and resolved, one is charged and occupied the other is neutral and unoccupied, c)  $[\text{H}_24^*]^{2+}$  (+2 charged rotaxane linker) showing two sites due to slow-exchange of occupied and unoccupied sites..

### Determination of Macrocycle Shuttling Rate in Solution

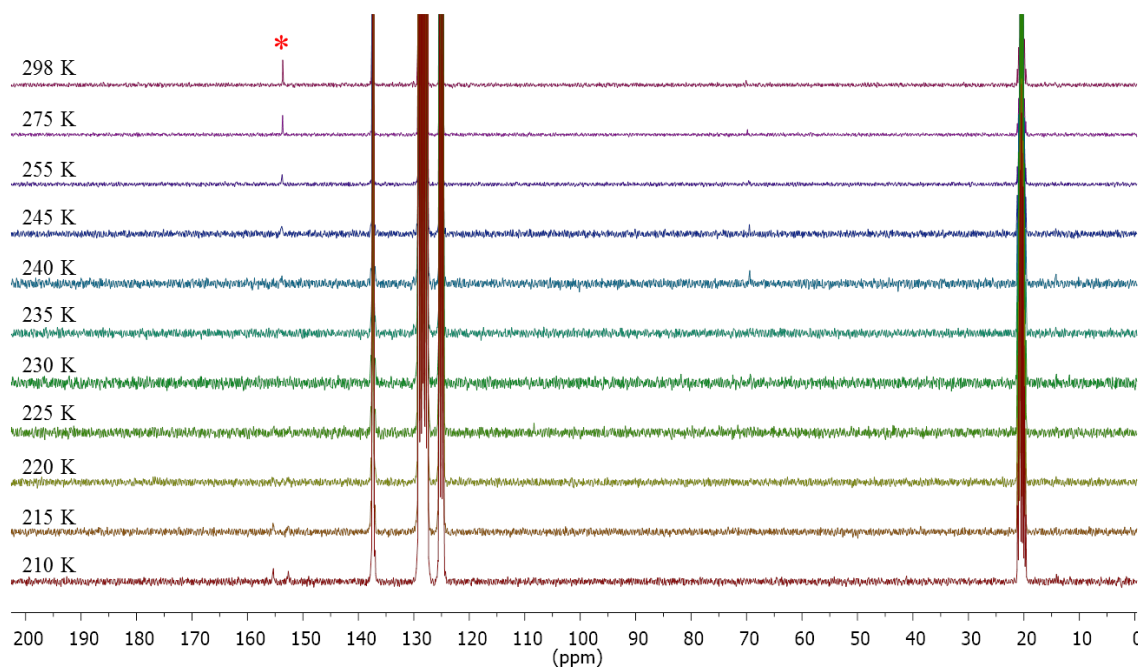


**Figure S26.** Variable temperature  $^{13}\text{C}$  NMR spectra of neutral  $4^*$  in toluene- $d_8$  (\* =  $^{13}\text{C}$ -enriched atoms, (toluene- $d_8$  was chosen as a solvent since it has both a low freezing point and low polarity).

The shuttling rates were calculated from a line shape analysis of the NMR spectra using the program DNMR71.EXE.<sup>S1</sup> Free energies of activation ( $\Delta G^\ddagger$ ) were estimated using the Eyring equation:  $\Delta G^\ddagger = -RT \ln(kh/k_B T)$ , where  $R$  is the ideal gas constant,  $h$  is Planck's constant and  $k_B$  is Boltzmann's constant. The enthalpic ( $\Delta H^\ddagger$ ) and entropic ( $\Delta S^\ddagger$ ) contributions to the transition state were calculated from Eyring plots:  $\ln(k/T) = -(\Delta H^\ddagger/RT) + (\Delta S^\ddagger/R) + \ln(k_B/h)$ .

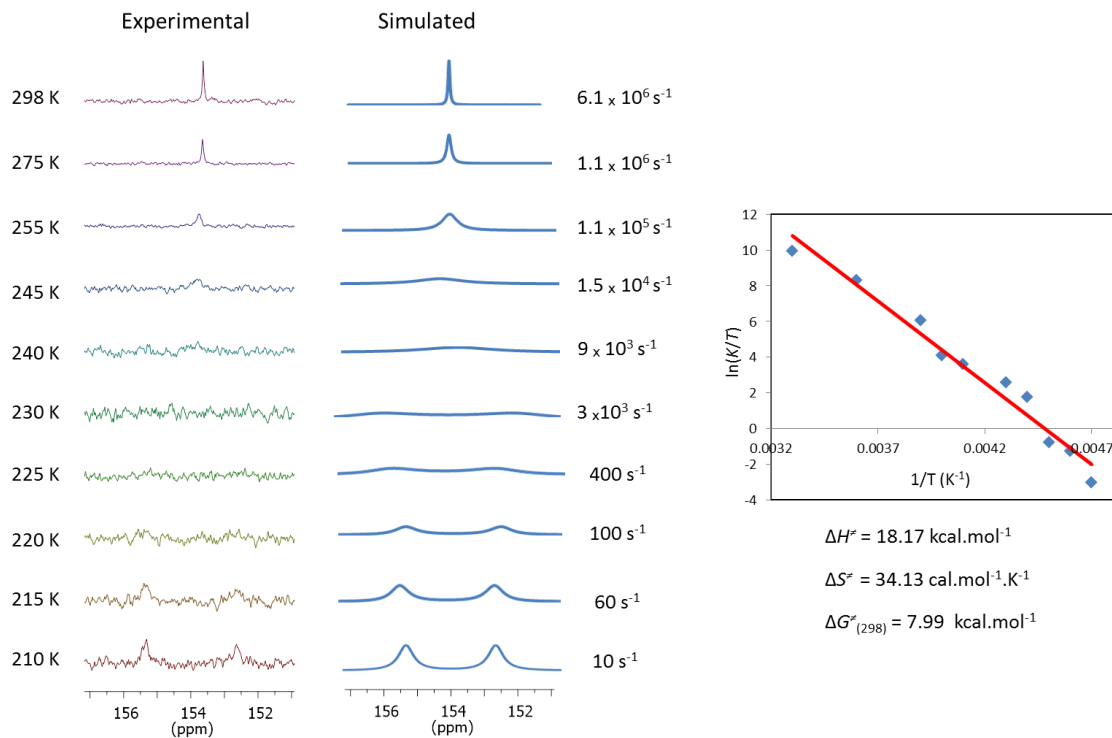


**Figure S27.** Comparison of the experimental and simulation  $^{13}\text{C}$  NMR data (left) for the  $^{13}\text{C}$ -enriched carbon of neutral **4\***, Eyring plot (right) for the shuttling of neutral **4\*** generated from the simulated data.

The shuttling rate for diprotonated **5\*** can be obtained from an EXSY experiment by using the equations shown below, where  $I_{AA}$  and  $I_{BB}$  are the diagonal peak intensities and  $I_{AB}$  and  $I_{BA}$  are the cross-peak intensities.  $k$  is the sum of the forward,  $k_1$ , and backward,  $k_{-1}$ , pseudo-first order rate constants for the shuttling process.  $k_1$  and  $k_{-1}$  are equal due to the identical stations and thus the observed pseudo-first order rate constant,  $k_{obs}$  can be determined.  $R$  is the ideal gas constant;  $h$  is Planck's constant and  $k_B$  is Boltzmann's constant.

$$r = I_{AA} + I_{BB}/I_{AB} + I_{BA}, \quad k = 1/\tau_m \ln(r + 1/r - 1), \quad k = k_1 + k_{-1}, \quad k_{obs} = k_1 = k_{-1}$$

$$\Delta G^\ddagger = -RT \ln(k_{obs} h/k_B T)$$

**Table S1.** Kinetic parameters for shuttling process of diprotonated **4\*** (no shuttling observed at 268 K).

$T$ (K)	$I_{AA}$	$I_{BB}$	$I_{AB}$	$I_{BA}$	$k_{obs}$ (S <sup>-1</sup> )	$\Delta G^\ddagger$ (kcal mol <sup>-1</sup> )
320 K	19889000	19369000	2539400	2826600	0.27	19.6
330 K	5104100	5035800	1031000	1375300	0.43	19.9

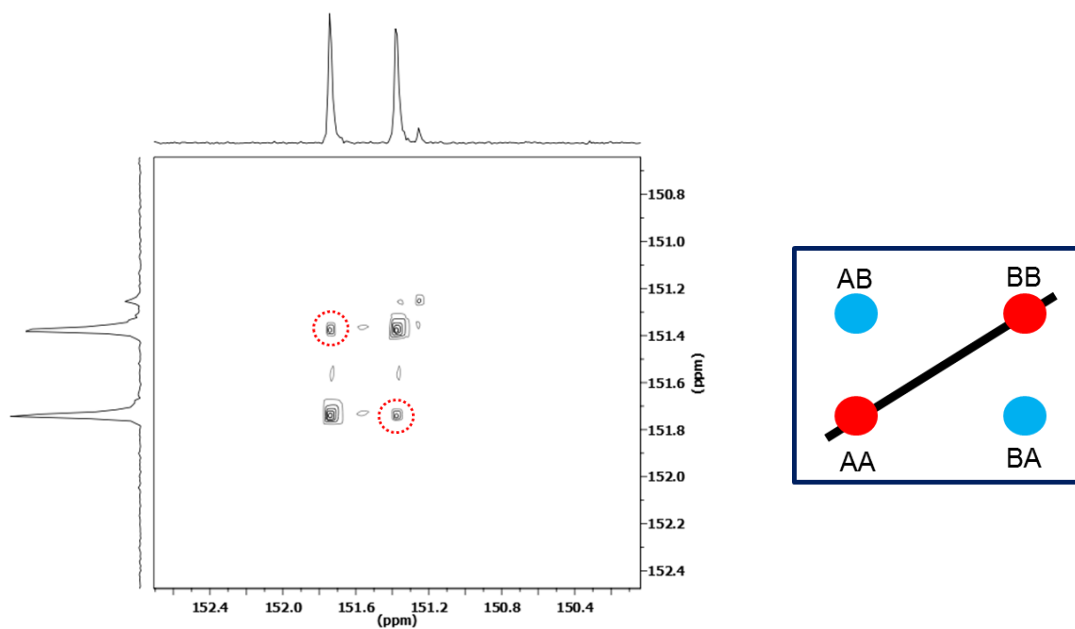


**Figure S28.** Partial 2D EXSY <sup>13</sup>C NMR (500 MHz, 320 K, CD<sub>3</sub>CN,  $\tau_m = 500$  ms) spectrum of diprotonated **4\***.



## Solution NMR Analysis of Digested MOFs

Samples were digested in a saturated D<sub>2</sub>O solution of K<sub>3</sub>PO<sub>4</sub>/d<sub>6</sub>-DMSO.

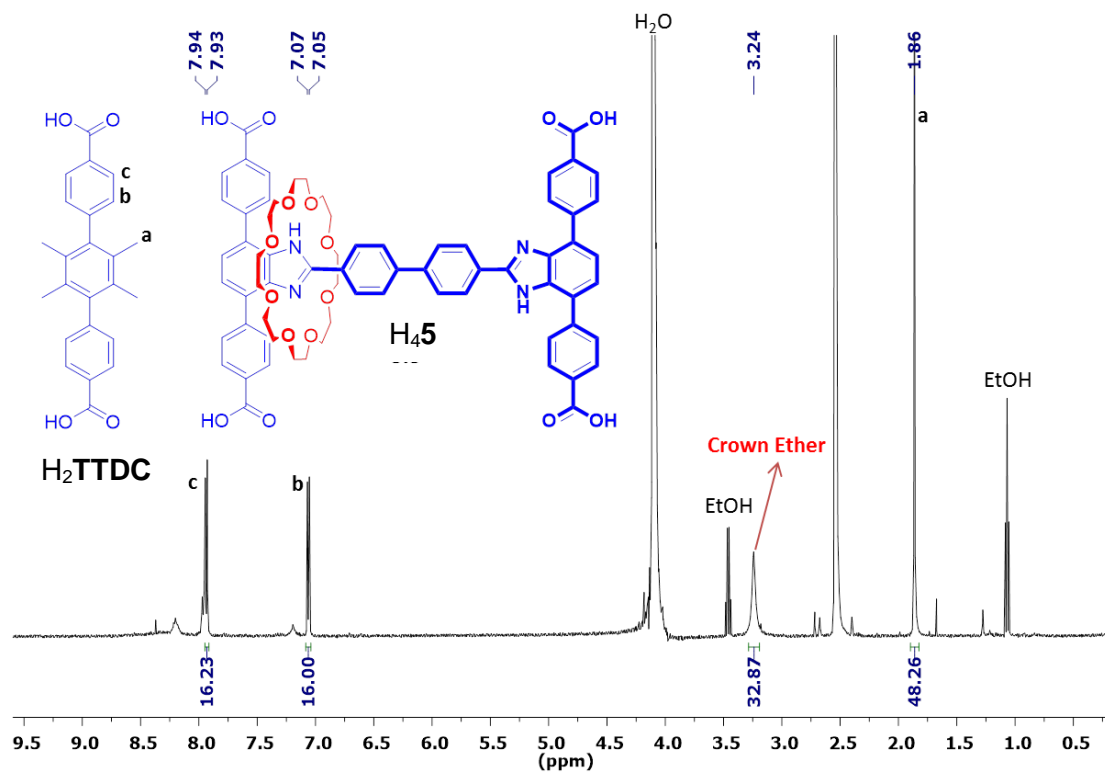


**Figure S29.** <sup>1</sup>H NMR of UWDM-8 after digestion (500 MHz, DMSO-d<sub>6</sub>), ratio of H<sub>2</sub>TTCP to 5\* is ~4:1.

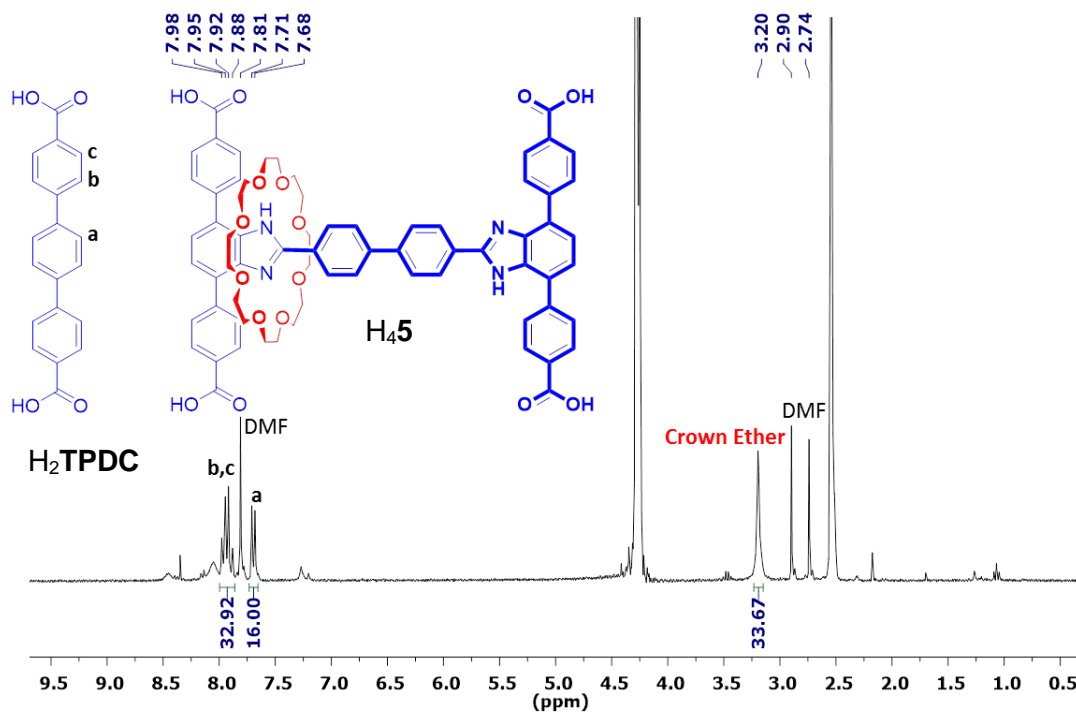


**Figure S30.** <sup>1</sup>H NMR of UWDM-9 after digestion (500 MHz, DMSO-d<sub>6</sub>), ratio of H<sub>2</sub>TPDC to H<sub>4</sub>5 is ~4:1.

## Solid-State NMR Analysis of MOF Synthesis

The presence of only a single peak for the carboxylic acid group (\*) in the  $^{13}\text{C}$  SSNMR spectra of known **PCN-57** and as-synthesized **UWDM-8** infers that all four of the carboxylate groups of the  $[\text{5}^*]^{4-}$  linker are incorporated into Zr-MOFs and bonded to Zr.

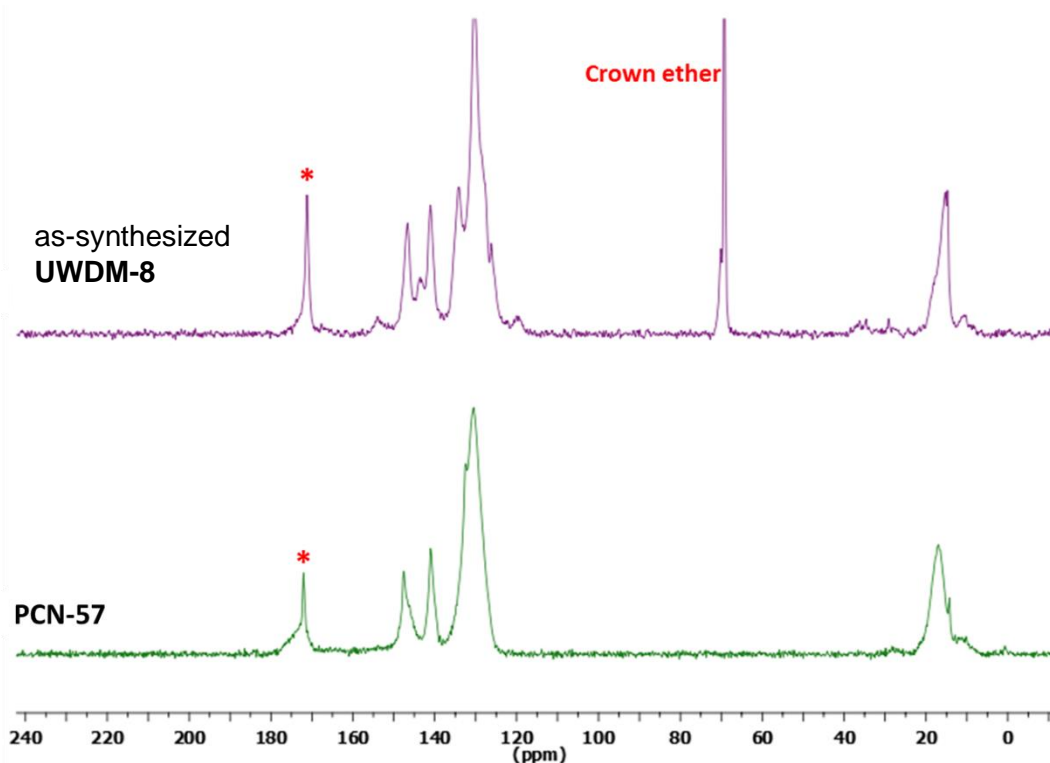


**Figure S31.**  $^{13}\text{C}$  SSNMR of as-synthesized **UWDM-8** and **PCN-57** (\* = carboxylic acid group).

## Synthesis of Various Protonation States of **4\***, **UWDM-8** and **UWDM-9**

Tetrafluoroboric acid diethyl ether complex (2  $\mu\text{L}$ , 0.015 mol) was added to a **4\*** (20 mg, 0.015 mmol) solution in  $\text{CH}_2\text{Cl}_2$  (2 mL). The mixture was stirred for 5 min. Ether was added to precipitate the product. The solids were filtered, washed with some ether and air dried giving to  $[\text{H}_2\mathbf{4}^*][\text{BF}_4]_2$ .

10 mg of  $[\text{H}_2\mathbf{4}^*][\text{BF}_4]_2$  dissolved in mixture of  $\text{CH}_3\text{CN}$  (2 mL) and  $\text{H}_2\text{O}$  (1 mL) and sonicated for 5 min. Then  $\text{CH}_3\text{CN}$  was removed, solids were filtered and air dried to yield  $[\text{H}\mathbf{4}^*][\text{BF}_4]$ .

The as-synthesized MOF,  $[\text{UWDM-8-H}][\text{CF}_3\text{CO}_2]$  (50 mg), was soaked in a 0.07 mol/L solution of proton sponge<sup>®</sup> (*N,N,N',N'*-tetramethyl-1,8-naphthalenediamine) in ethanol (60 mg in 4 mL EtOH). The mixture was kept in the dark at room temperature for 72 h (solvent replaced every 12 h and the qualitative level of deprotonation was monitored by UV irradiation). The crystals were then washed with fresh ethanol once and re-soaked in fresh ethanol for 2 h. The solids were filtered, air-dried and were activated at 160  $^\circ\text{C}$  for 12 h giving to **UWDM-8**.

25 mg of **UWDM-8** was soaked in a 2 M solution of  $\text{CF}_3\text{SO}_3\text{H}$  in ethanol at 60  $^\circ\text{C}$  for 24 h (solvent replaced every 12 h). The microcrystals were filtered, washed with ethanol, air dried and were activated at 160  $^\circ\text{C}$  for 12 h to give  $[\text{UWDM-8-H}_2][\text{OTf}]_2$ . The same methods were used for **UWDM-9**. The results of optical microscope images (Fig S32) of three states of **UWDM-9** were similar to **UWDM-8**.

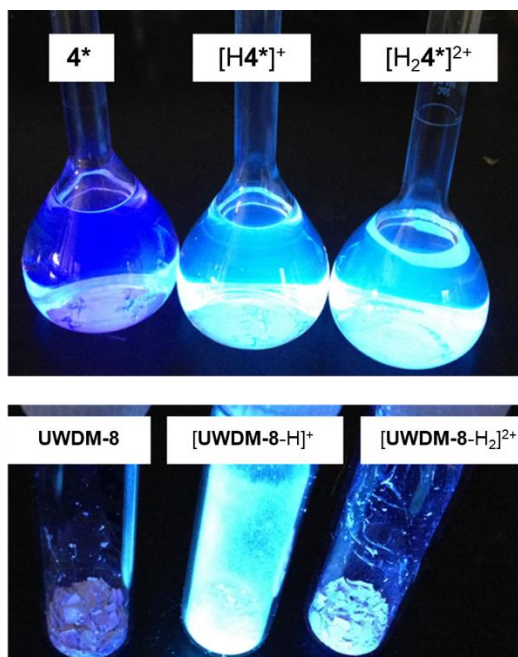


**Figure S32.** Optical microscope images of the three protonation states of 4\* linkers in CD<sub>2</sub>Cl<sub>2</sub> and microcrystals of UWDM-8 under UV irradiation.

#### VT PXRD for UWDM-8 and UWDM-9

Powder X-ray diffraction (PXRD) measurements were recorded on a Brüker D8 Discover diffractometer equipped with a GADDS 2D-detector and operated at 40 kV and 40 mA. CuK $\alpha$  radiation ( $\lambda = 1.54187 \text{ \AA}$ ) was used and the initial beam diameter was 0.5 mm. Samples were mounted in a 0.5 mm boron-rich capillary tube on a goniometer head. Data was collected as rotation frames at  $2\theta$  value of  $18^\circ$  for 15 min.

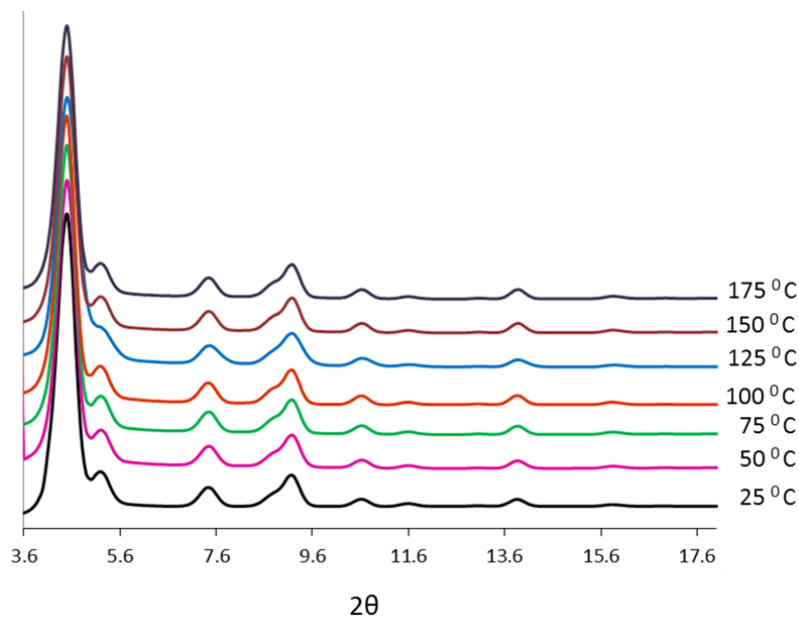


**Figure S33.** Variable temperature PXRD analysis of UWDM-8.

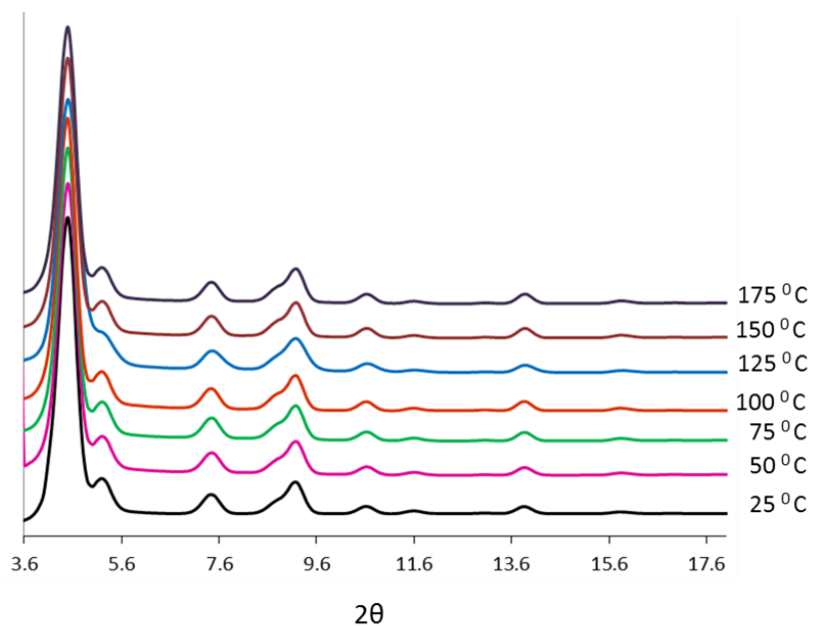


**Figure S34.** VT PXRD analysis of **UWDM-9**.

### VT $^{13}\text{C}$ MAS SSNMR Spectra of UWDM-8 and UWDM-9

#### UWDM-8

(based on PCN-57)

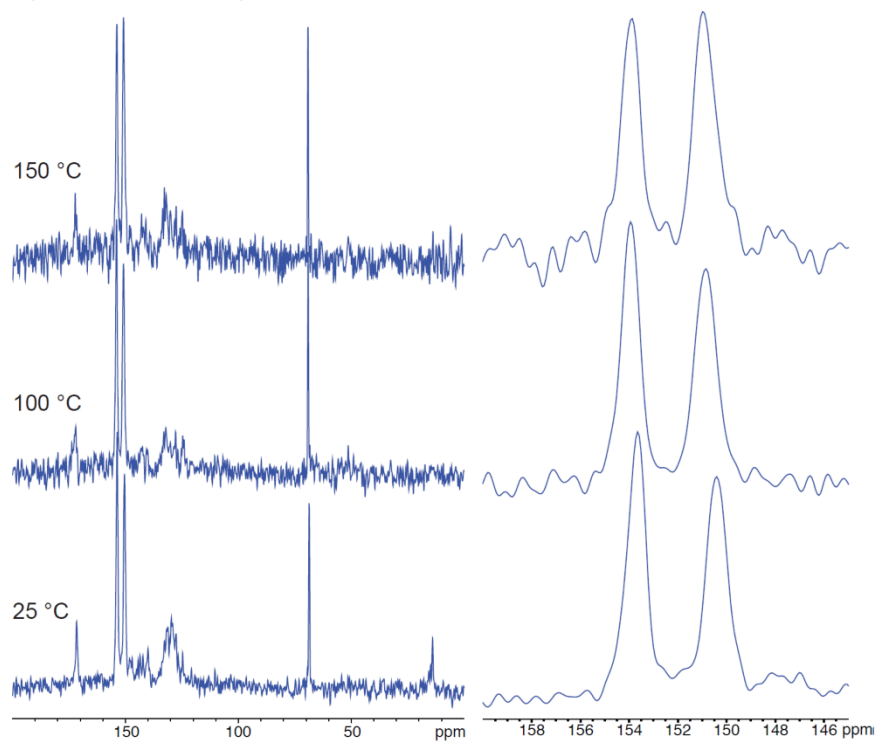


**Figure S35.** Variable temperature CP MAS  $^{13}\text{C}$  SSNMR analysis of **UWDM-8**. The temperature was increased in an attempt to induce exchange between the two sites.

**UWDM-9**  
(based on UiO-68)

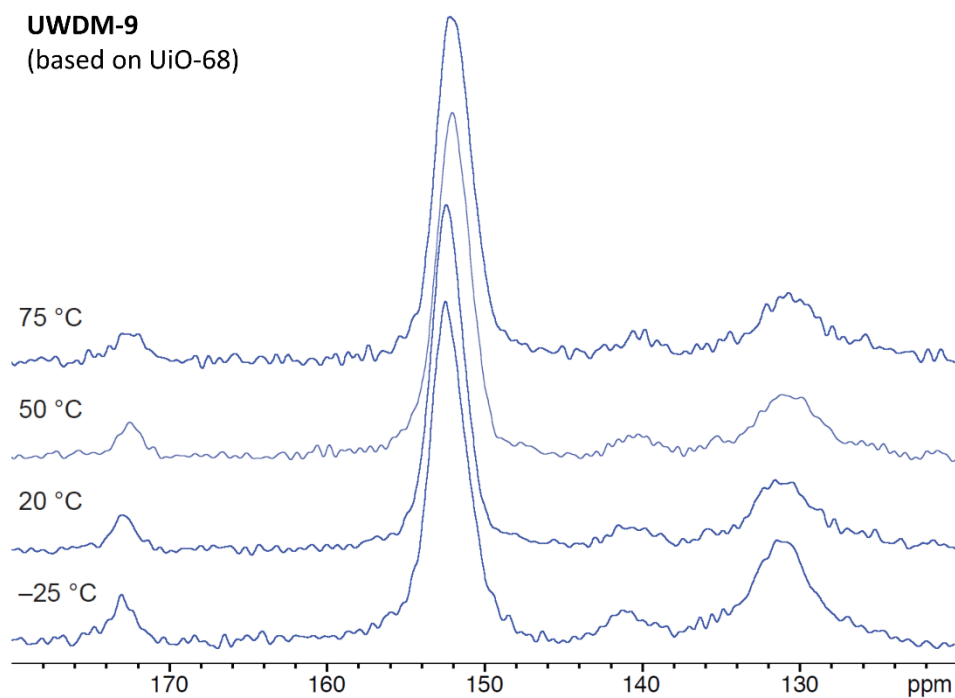


**Figure S36.** VT CP MAS  $^{13}\text{C}$  SSNMR analysis of **UWDM-9**. The temperature was lowered in an attempt to freeze out the limiting chemical shifts.

## References

1. Reich, H. J., DNMR71.EXE. *J. Chem. Educ. Software* **1996**.